JOC Article

Enthalpy (ΔH) and Entropy (ΔS) for π-Stacking Interactions in Near-Sandwich Configurations: Relative Importance of Electrostatic, Dispersive, and Charge-Transfer Effects

Benjamin W. Gung,* Xiaowen Xue, and Yan Zou

Department of Chemistry & Biochemistry, Miami University, Oxford, Ohio 45056

gungbw@muohio.edu

Received December 10, 2006

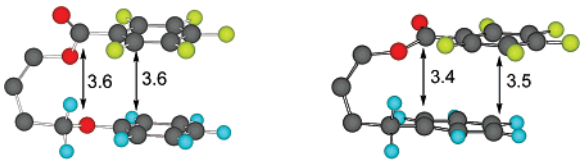

(a) Sandwich (b) Parallel-displaced

Interactions between two aromatic rings with various substituents in a near-sandwich configuration have been quantitatively studied by using the triptycene derived molecular models. This model system allows a stacking arrangement of two arenes to assume a near-perfect face-to-face configuration in its ground state conformation. Comparing to our previous study of the parallel displaced configuration, repulsive interactions are predominant for most arenes currently studied. However, if one arene is strongly electron deficient (Ar_2 = pentafluorobenzoate), attractive interactions were observed regardless of the character of the other arene (Ar_1). For stacking interactions between $Me_2NC_6H_4$ and C_6F_5CO groups, a ΔH of -1.84 ± 0.2 kcal/mol and a ΔS of -2.9 ± 0.8 cal/(mol·K) were determined. The general trend in the attractive stacking interaction toward a pentafluorobenzoate is $Me_2NC_6H_4 > Me_3C_6H_2 > Me_2C_6H_3 > MeC_6H_4 > MeOC_6H_4 > C_6H_5 > O_2NC_6H_4$. The observed trend is consistent with a donor−acceptor relationship and the acceptor is a C_6F_5CO group.

Introduction

Aromatic interactions play important roles in biological recognition and crystal engineering.[1,2] Widespread interest have been shown in the development of models to improve our understanding of these interactions.[3−5] The two most noted models with strategies to quantify aromatic interactions in the stacking conformation include the 1,8-diarylnaphthalene system by Cozzi, Siegel, and co-workers and the double mutant cycle system by Hunter and co-workers.[6−9] However, each model system has its limitations and the previous models were either too restrictive or too flexible.[8−11] There have not been enough quantitative studies to compare and reach a generally agreed value for the magnitude of aromatic interactions in solution.[5] Other studies involving the edge-to-face conformation have been

(1) Kool, E. T.; Morales, J. C.; Guckian, K. M. Mimicking the structure and function of DNA: Insights into DNA stability and replication. *Angew. Chem., Int. Ed.* **2000**, *39*, 990−1009.

(2) Coates, G. W.; Dunn, A. R.; Henling, L. M.; Dougherty, D. A.; Grubbs, R. H. Phenyl-perfluorophenyl stacking interactions: a new strategy for supermolecule construction. *Angew. Chem., Int. Ed. Engl.* **1997**, *36*, 248−251.

(3) Hunter, C. A.; Lawson, K. R.; Perkins, J.; Urch, C. J. Aromatic interactions. *J. Chem. Soc., Perkin Trans. 2* **2001**, 651−669.

(4) Waters, M. L. Aromatic interactions in model systems. *Curr. Opin. Chem. Biol.* **2002**, *6*, 736−741.

(5) Meyer, E. A.; Castellano, R. K.; Diederich, F. Interactions with aromatic rings in chemical and biological recognition. *Angew. Chem., Int. Ed.* **2003**, *42*, 1210−1250.

(6) Cozzi, F.; Cinquini, M.; Annunziata, R.; Dwyer, T.; Siegel, J. S. Polar/π Interactions between Stacked Aryls in 1,8-Diarylnaphthalenes. *J. Am. Chem. Soc.* **1992**, *114*, 5729−5733.

(7) Cozzi, F.; Cinquini, M.; Annuziata, R.; Siegel, J. S. Dominance of Polar/π over Charge-Transfer Effects in Stacked Phenyl Interactions. *J. Am. Chem. Soc.* **1993**, *115*, 5330−5331.

(8) Adams, H.; Blanco, J. L.; Chessari, G.; Hunter, C. A.; Low, C. M.; Sanderson, J. M.; Vinter, J. G. Quantitative determination of intermolecular interactions with fluorinated aromatic rings. *Chem.−Eur. J.* **2001**, *7*, 3494−3503.

(9) Cockroft, S. L.; Hunter, C. A.; Lawson, K. R.; Perkins, J.; Urch, C. J. Electrostatic Control of Aromatic Stacking Interactions. *J. Am. Chem. Soc.* **2005**, *127*, 8594−8595.

(10) Schneider, H. J. Requirements for quantifications of weak intermolecular interactions from equilibrium studies with supramolecular complexes. *Angew. Chem., Int. Ed. Engl.* **1997**, *36*, 1072−1073.

(11) Martinez, A. G.; Barcina, J. O.; Cerezo, A. D. Influence of highly preorganised 7,7-diphenylnorbornane in the free energy of edge-to-face aromatic interactions. *Chem.-Eur. J.* **2001**, *7*, 1171−1175.

10.1021/jo062526t CCC: $37.00
Published on Web 03/06/2007

reported.[12−14] This study is focused on the face-to-face or sandwich configuration.

Recently we reported our studies on aromatic interactions using the triptycene derived model system,[15,16] which allows the arenes to interact near their van der Waals' contact, and quantitative determination of the magnitude of interaction was achieved. Our previous study involved arene−arene interactions in the parallel displaced configurations (**1**), i.e., the two arenes are parallel to each other with the center of one arene on top of the edge of the other. Through molecular modeling, we have found that by a small modification to the previous model compound, the arenes can be arranged to assume a near-sandwich configuration in the *syn* rotamer of **2**.

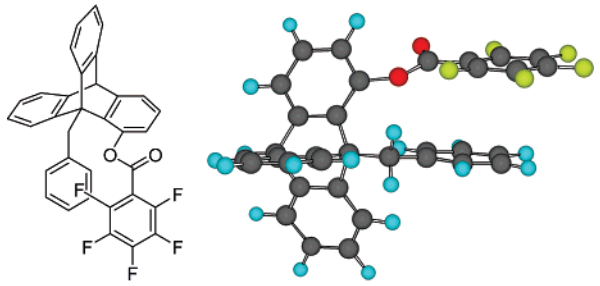

1 Parallel displaced

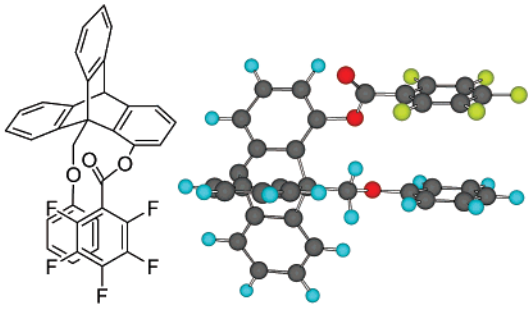

2 Sandwich

Currently few experimental data are available on the magnitude of arene interactions in solution. Although the significant role played by quadrupole moments of benzene and hexafluorobenzene has been elegantly presented,[17−20] it seems that no agreement has been reached on whether electrostatic interactions alone control aromatic interactions.[5] The consideration of quadrupole moments provides a simple way to visualize the charge distribution of aromatics and correctly predicts the preferred geometry of symmetrically substituted arene interactions. However, if the arenes are stacked at van der Waals distance, it would not be appropriate for the interactions to be quantitatively modeled as just a quadrupole−quadrupole interaction.[20,21] In fact, recent high-level theoretical studies have indicated that electrostatic forces alone cannot rationalize the energetic ordering of substituent effects.[22] In general, theoretical studies have demonstrated the importance of dispersive forces.[5] Our study has shown that in addition to electrostatic and dispersive forces, charge-transfer or donor−acceptor interactions also play a role in aromatic interactions.[16] We have recently reported the observation that a charge-transfer band was observed in the stacking interactions between a *N*,*N*-dimethylaminophenyl group and a pentafluorobenzoate group in a parallel-displaced configuration.[16] This study shows that charge-transfer interactions are also present for the same arene pair in a near-sandwich configuration. Our data are consistent with the view that electrostatic, dispersive, and donor−acceptor forces all play a role in aromatic interactions in organic solvents. The relative importance of each force depends on the characteristics of the two arenes involved.

Results

As a result of molecular modeling studies, a modification to our recently reported model compounds was made in order to study aromatic interactions in the sandwich configuration. This calls for an insertion of an oxygen atom into our previous model between the bridgehead (C9) CH_2 group and the phenyl group. The compounds used in this study and their syntheses are summarized in Scheme 1. We will briefly describe the synthetic procedures.

Synthesis of the Model Compounds. The preparation of the desired compounds **6a**−**12i** started with a Diels−Alder reaction. Various anthraceny ethers **3** were prepared according to literature procedures[23,24] and were allowed to react with the dienophile *p*-benzoquinone. The Diels−Alder reaction was followed by an equilibration/aromatization with KOAc to produce the triptycene derivative **4**. The less sterically hindered phenolic OH group at C4 was protected by a pivaloyl group to produce ester **5**. The pivaloyl group was chosen to be the spectator group to increase the solubility of these model compounds. The synthesis was completed with acylation reaction with substituted benzoyl chloride Ar_2COCl to afford the desired model compounds **6a**−**12i**.

(12) Paliwal, S.; Geib, S.; Wilcox, C. S. Chemistry of Synthetic Receptors and Functional-Group Arrays. 24. Molecular Torsion Balance for Weak Molecular Recognition Forces−Effects of Tilted-T Edge-to-Face Aromatic Interactions on Conformational Selection and Solid-State Structure. *J. Am. Chem. Soc.* **1994**, *116*, 4497−4498.

(13) Kim, E.; Paliwal, S.; Wilcox, C. S. Measurements of molecular electrostatic field effects in edge-to-face aromatic interactions and CH-π interactions with implications for protein folding and molecular recognition. *J. Am. Chem. Soc.* **1998**, *120*, 11192−11193.

(14) Jennings, W. B.; Farrell, B. M.; Malone, J. F. Attractive intramolecular edge-to-face aromatic interactions in flexible organic molecules. *Acc. Chem. Res.* **2001**, *34*, 885−894.

(15) Gung, B. W.; Xue, X. W.; Reich, H. J. The strength of parallel-displaced arene−arene interactions in chloroform. *J. Org. Chem.* **2005**, *70*, 3641−3644.

(16) Gung, B. W.; Patel, M.; Xue, X. W. A threshold for charge transfer in aromatic interactions? A quantitative study of π-stacking interactions. *J. Org. Chem.* **2005**, *70*, 10532−10537.

(17) Williams, J. H. The Molecular Electric Quadrupole-Moment and Solid-State Architecture. *Acc. Chem. Res.* **1993**, *26*, 593−598.

(18) Luhmer, M.; Bartik, K.; Dejaegere, A.; Bovy, P.; Reisse, J. The Importance Of Quadrupolar Interactions In Molecular Recognition Processes Involving A Phenyl Group. *Bull. Soc. Chim. Fr.* **1994**, *131*, 603−606.

(19) Cozzi, F.; Ponzini, F.; Annunziata, R.; Cinquini, M.; Siegel, J. S. Polar interactions between stacked p systems in fluorinated 1,8-diarylnaphthalenes: importance of quadrupole moments in molecular recognition. *Angew. Chem., Int. Ed. Engl.* **1995**, *34*, 1019−1020.

(20) Ma, J. C.; Dougherty, D. A. The cation-π interaction. *Chem. Rev.* **1997**, *97*, 1303−1324.

(21) Gung, B. W.; Amicangelo, J. C. Substituent Effects in C_6F_6-C_6H_5X Stacking Interactions. *J. Org. Chem.* **2006**, *71*, 9261−9270.

(22) Sinnokrot, M. O.; Sherrill, C. D. Substituent effects in π-π interactions: Sandwich and T-shaped configurations. *J. Am. Chem. Soc.* **2004**, *126*, 7690−7697.

(23) Tamura, Y.; Yamamoto, G.; Oki, M. CH_3-O hydrogen bond. Implications of its presence from the substituent effects on the populations of rotamers in 4-substituted 9-ethyl-1-methoxytriptycenes and 9-(substituted phenoxymethyl)-1,4-dimethyltriptycenes. *Bull. Chem. Soc. Jpn.* **1987**, *60*, 1781−1788.

(24) Kimura, N. The Role of the Leaving Group in the Dissociation of Radical Anions of 9-(Aryloxymethyl)anthracenes. *J. Am. Chem. Soc.* **2001**, *123*, 3824−3825.

SCHEME 1

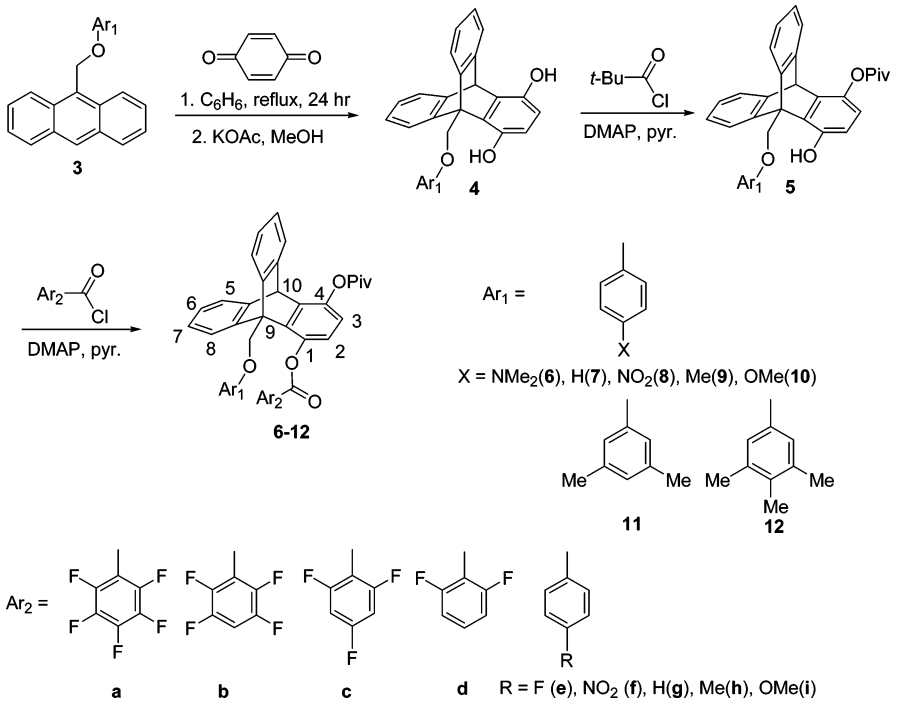

Conformations of the *Syn* and *Anti* Isomers. The two arenes are denoted as Ar_1 and Ar_2 with Ar_1 attached to the bridgehead carbon (C9) and Ar_2 attached to C1 of the triptycene system. Ar_1 and Ar_2 are face-to-face and within van der Waals' contact distance in the *syn* conformation (Figure 1(a)). In the anti conformation, the Ar_1 group bisects the triptycene skeleton and the Ar_2 group assumes the perpendicular arrangement from the triptycene skeleton (Figure 1(b)). It appears to be an edge-to-face arrangement between Ar_1 and Ar_2 in the anti conformation. However, the distance between the C−H of Ar_1 and the π-face of Ar_2 is not optimal and the substituent effects do not correlate with the potential edge-to-face interaction in the anti conformation. As shown in Scheme 1, the Ar_1 groups range from monosubstituted *p*-X-phenyl to multiple methyl-substituted phenyl groups. The substituent X is varied from a strongly electron-donating group such as NMe_2 to an electron-withdrawing group such as NO_2. The Ar_2 groups also involve both monosubstituted benzoate and an increasingly electron-deficient arene by the increase of fluorine atoms on the aromatic ring. Molecular modeling via MacroModel (version 7.0; force field: MMFFs) shows a stable near-sandwich configuration between Ar_1 and Ar_2 in model compound **7a** where $Ar_2 = C_6F_5$, Figure 1. It is important to point out that the structures shown here were modeled by molecular mechanics, therefore, the sandwich conformation is stable based on steric and electrostatic effects alone. Other electronic effects such as dispersion forces can only be estimated by using more sophisticated electronic models. The only apparent repulsive close contact in the *syn* conformation (Figure 1, structure in part a) is between the oxygen atom at C1 and the one at the bridgehead CH_2. The arenes are far enough from each other in the *anti* conformer (Figure 1, structure in part b) that neither steric and nor stacking interactions are present. The only potential interaction between Ar_1 and Ar_2 in the anti conformation is the attractive edge-to-face interaction mentioned above. Therefore any preference for the *syn* conformation should be the results of attractive interactions from the stacking orientation rather than repulsions from the anti conformer.

Variable-Temperature NMR Spectroscopy A variable-temperature NMR study was carried out with these model compounds. Two conformational isomers, the *syn* and the *anti*, can be observed at low temperatures. This is due to the slow rotation of the bridgehead CH_2 group in these compounds on the NMR time scale, which allows the integration and the determination of the *syn*/*anti* isomer ratio for each compound (Figure 2). It is important to point out that the conformational freedom is rather limited for either the *anti* or the *syn* isomers. The C1 ester linkage prefers the *s*-trans conformation (Figure 1) by ~4.5 kcal/mol to the alternative *s*-cis conformation to avoid oxygen lone pair repulsion.[25,26] Furthermore, the $Ar_2C(=O)-O$ bond prefers to be nearly perpendicular to the triptycene arene plane, which allows a parallel alignment between Ar_1 and Ar_2, Figure 1. Thus the *syn*/*anti* ratio is effectively the equilibrium constant between the stacked (or syn) and the separated (or anti) arene conformations. Since statistically two *syn* and one *anti* conformer are expected, the equilibrium constant, K_{eq}, should be 1/2•*syn*/*anti* ratio. The Ar_1OCH_2 protons are diastereotopic in the *syn* conformational isomer and display an *AB* quartet while they are enantiomeric in the *anti* conformation and appear as a singlet. The experimentally determined *syn*/*anti* ratios in $CDCl_3$ at different temperatures are shown in Table 1.

The ratio changes significantly with temperature when a model compound displays a large *syn*/*anti* ratio. This enables

(25) Glaser, R. Aspirin. An ab Initio Quantum-Mechanical Study of Conformational Preferences and of Neighboring Group Interactions. *J. Org. Chem.* **2001**, *66*, 771−779.

(26) Gung, B. W.; Xue, X. W.; Reich, H. J. Off-center oxygen-arene interactions in solution: A quantitative study. *J. Org. Chem.* **2005**, *70*, 7232−7237.

(27) Shoemaker, D. P.; Garland, C. W.; Nibler, J. W. *Experiments in Physical Chemistry*, 6th ed.; McGraw-Hill: New York, 1996.

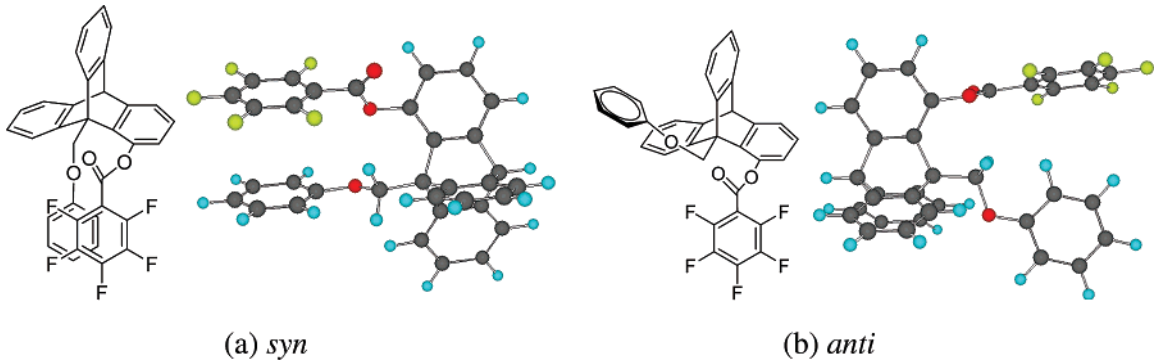

FIGURE 1. Global ground state conformations for (a) *syn* and (b) *anti* isomers. Ar_1 = phenyl, Ar_2 = pentafluorobenzoate.

us to obtain both ΔH and ΔS by using the van't Hoff eq 1. Considering the importance of entropic effects in noncovalent interactions,[11] this study provides information for π-stacking that has not been reported from previous systems. Thermodynamic parameters are collected in Tables 2−4. Some caution should be taken with these data since the enthalpy and entropy obtained with use of the van't Hoff equation assume a constant enthalpy value in the surveyed temperature range, which may or may not be true.

$$\ln K_{eq} = -\Delta H°/RT + \Delta S°/R \qquad (1)$$

where K_{eq} = 1/2·*syn*/*anti* and R is the gas constant.

Discussion

As shown in Table 1, the largest *syn*/*anti* ratio was obtained for compound **6a**, where Ar_1 = $C_6H_4NMe_2$ and Ar_2 = C_6F_5. This corresponds to a ΔH of −1.84 ± 0.2 kcal/mol and a ΔS of −2.86 ± 0.83 cal/(mol·K) (Table 2) in favor of the stacking configuration. Hunter and co-workers have reported a study for a pair of arenes with similar structures using their chemical double mutant model system.[8] Only room temperature study was conducted and a free energy of 0.4 kcal/mol was deduced for the stacking interactions between pentafluoro-aminophenyl and *N*,*N*-dimethylaminobenzoate grouping (see below) in $CDCl_3$. From our experiments, the ΔH and ΔS in Table 2 give a free energy of 0.99 ± 0.2 kcal/mol at 293 K in the same solvent.

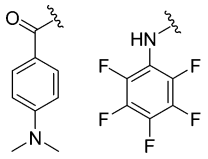

(a) arenes used in ref. 8

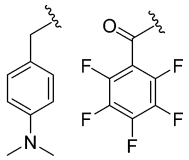

(b) arenes in **6a**

The difference in the structures between that used in Hunter's experiments and the current experiment may partially account for the difference in observed free energies. The donor and acceptor groups in our model system are more electron-rich and -deficient, respectively, than that used in Hunter's experiments. This difference in arene structures may well account for the fact that the attractive interactions in our model system are twice as strong as that determined by the chemical double mutant cycle experiments. Double mutant cycle experiments offer a sophisticated and laborious approach to dissecting a complex system to a single weak interaction. However, the method suffers in accuracy as suggested previously,[10,11] because the flexibility of

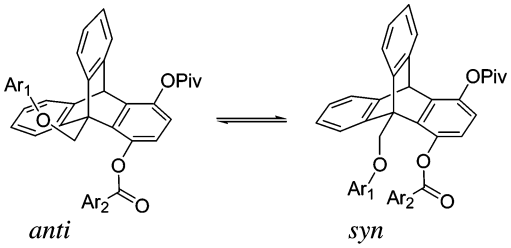

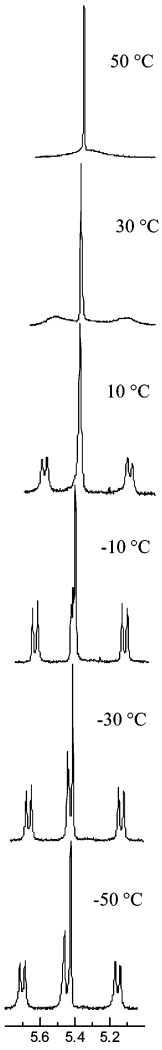

FIGURE 2. The temperature-dependent NMR signals (300 MHz in $CDCl_3$) from the bridgehead $C(9)H_2$ protons of compound **7f**. The sharp singlet is the bridgehead CH at C10.

TABLE 1. Ratios of *Syn*/*Anti* Isomers at Different Temperatures for Model Compounds 6a−14a[a]

				syn/anti ratio in $CDCl_3$ at different temperatures (°C)				
entry	compd	Ar_1	Ar_2	−10	−20	−30	−40	−50
1	**6a**	$C_6H_4NMe_2$	C_6F_5	15.7	17.5	20.7	26.5	28.0
2	**6b**	$C_6H_4NMe_2$	C_6HF_4	5.37	6.04	6.61	7.36	8.87
3	**6c**	$C_6H_4NMe_2$	$C_6H_2F_3$	1.62	1.70	1.83	1.90	1.93
4	**6d**	$C_6H_4NMe_2$	$C_6H_3F_2$	0.72	0.71	0.72	0.72	0.74
5	**6e**	$C_6H_4NMe_2$	C_6H_4F	0.54	0.53	0.48	0.47	0.47
6	**7a**	C_6H_5	C_6F_5	11.0	11.7	13.7	15.7	18.0
7	**7f**	C_6H_5	$C_6H_4NO_2$	2.63	2.78	2.94	3.08	3.27
8	**7e**	C_6H_5	C_6H_4F	0.55	0.54	0.53	0.50	0.47
9	**7g**	C_6H_5	C_6H_5	0.30	0.29	0.26	0.24	0.21
10	**7h**	C_6H_5	C_6H_4Me	0.19	0.17	0.16	0.14	0.12
11	**7i**	C_6H_5	C_6H_4OMe	0.23	0.22	0.19	0.18	0.17
12	**8a**	$C_6H_4NO_2$	C_6F_5	5.6	6.0	6.8	7.6	8.9
13	**8f**	$C_6H_4NO_2$	$C_6H_4NO_2$	2.66	2.73	2.85	2.94	3.05
14	**8e**	$C_6H_4NO_2$	C_6H_4F	0.96	0.92	0.90	0.89	0.89
15	**8g**	$C_6H_4NO_2$	C_6H_5	0.59	0.56	0.55	0.53	0.50
16	**8h**	$C_6H_4NO_2$	C_6H_4Me	0.54	0.51	0.48	0.46	0.44
17	**8i**	$C_6H_4NO_2$	C_6H_4OMe	0.61	0.59	0.57	0.54	0.52
18	**9a**	C_6H_4Me	C_6F_5	13.5	15.2	17.2	18.7	21.3
19	**10a**	C_6H_4OMe	C_6F_5	10.6	12.0	13.1	15.8	18.2
20	**11a**	$C_6H_3Me_2$	C_6F_5	15.2	17.5	19.8	21.0	23.3
21	**12a**	$C_6H_2Me_3$	C_6F_5	17.1	19.1	21.3	23.8	26.1
22	**13**	C_6H_4Me	CH_3	1.99	2.08	2.27	2.40	2.58
23	**14**	CH_3	CH_3	0.32	0.32	0.30	0.28	0.27

[a] The experiments were performed in $CDCl_3$ unless stated otherwise.

TABLE 2. The Effect of the Number of Fluorine Atoms of Ar_2 on ΔH and ΔS for Arene−Arene Interactions in $CDCl_3$[a]

entry	compd	Ar_1	Ar_2	$\Delta H°_{anti\rightarrow syn}$,[b]	$\Delta S°_{anti\rightarrow syn}$[c]	$\Delta G_{anti\rightarrow syn}$[d]
1	**6a**	$C_6H_4NMe_2$	C_6F_5	-1.84 ± 0.2	-2.9 ± 0.8	-0.99 ± 0.2
2	**6b**	$C_6H_4NMe_2$	C_6HF_4	-1.41 ± 0.1	-3.4 ± 0.3	-0.41 ± 0.1
3	**6c**	$C_6H_4NMe_2$	$C_6H_2F_3$	-0.53 ± 0.1	-2.4 ± 0.3	-0.17 ± 0.1
4	**6d**	$C_6H_4NMe_2$	$C_6H_3F_2$	-0.08 ± 0.1	-2.4 ± 0.2	0.62 ± 0.1
5	**6e**	$C_6H_4NMe_2$	C_6H_4F	0.46 ± 0.1	-0.9 ± 0.5	0.72 ± 0.1

[a] The standard errors are calculated by using linear regression analysis.[27] [b] In units of kcal/mol. [c] In units of cal/(mol·K). [d] In units of kcal/mol at 293 K.

TABLE 3. Substituent Effect on the ΔH and ΔS for Arene−Arene Interactions[a]

entry	compd	Ar_1	Ar_2	$\Delta H°_{anti\rightarrow syn}$[b,c]	$\Delta S°_{anti\rightarrow syn}$[b,d] in $CDCl_3$
1	**7a**	C_6H_5	C_6F_5	-1.49 ± 0.08	-2.3 ± 0.3
2	**7f**	C_6H_5	$C_6H_4NO_2$	-0.63 ± 0.02	-1.8 ± 0.1
3	**7e**	C_6H_5	C_6H_4F	0.46 ± 0.06	-0.8 ± 0.3
4	**7g**	C_6H_5	C_6H_5	1.06 ± 0.1	0.3 ± 0.4
5	**7h**	C_6H_5	C_6H_4Me	1.30 ± 0.1	0.3 ± 0.4
6	**7i**	C_6H_5	C_6H_4OMe	0.93 ± 0.1	-0.8 ± 0.5
7	**8a**	$C_6H_4NO_2$	C_6F_5	-1.36 ± 0.1	-3.2 ± 0.3
8	**8f**	$C_6H_4NO_2$	$C_6H_4NO_2$	-0.41 ± 0.1	-1.0 ± 0.1
9	**8e**	$C_6H_4NO_2$	C_6H_4F	0.21 ± 0.1	-0.7 ± 0.3
10	**8g**	$C_6H_4NO_2$	C_6H_5	0.45 ± 0.1	-0.7 ± 0.2
11	**8h**	$C_6H_4NO_2$	C_6H_4Me	0.59 ± 0.1	-0.4 ± 0.2
12	**8i**	$C_6H_4NO_2$	C_6H_4OMe	0.48 ± 0.1	-0.6 ± 0.1

[a] The standard errors are calculated by using linear regression analysis.[27] [b] Negative values indicate attractive and positive values repulsive interactions. [c] In units of kcal/mol. [d] In units of cal/(mol·K).

TABLE 4. Comparison between Sandwich and Parallel-Displaced *π*-Stacking

				ratio (*syn*/*anti*, at −15 °C)	
entry	compd	Ar_1	Ar_2	sandwich[a]	parallel-displaced[b]
1	**6a**	$C_6H_4NMe_2$	C_6F_5	16.6	21.7
2	**10a**	C_6H_4OMe	C_6F_5	11.2	16.8
3	**7a**	C_6H_5	C_6F_5	11.3	13.7
4	**7f**	C_6H_5	$C_6H_4NO_2$	2.71	9.0
5	**7e**	C_6H_5	C_6H_4F	0.55	2.9
6	**7g**	C_6H_5	C_6H_5	0.30	1.9
7	**7i**	C_6H_5	C_6H_4OMe	0.23	1.7

[a] This work. [b] Reference 16.

the system and the uncertainty was multiplied because four different binding studies were required.

The entropies for edge-to-face interactions have been determined by Jennings and co-workers.[14] However, to our knowledge, the entropies for stacking aromatic interactions are for the first time determined experimentally. The entropy values shown in Tables 2 and 3 are significantly negative when the interactions are strongly attractive. On the other hand, negligible or positive values are obtained when the interactions are small or repulsive. Thus to a certain degree, an enthalpy−entropy compensation is shown in this conformational equilibrium.[28] However, the entropy decrease does not completely offset the enthalpy gained through substituent effects. This is evidenced by the different free energies observed for different arene pairs. The errors associated with the entropy values should be greater than the corresponding enthalpy values since the ΔS is derived from the intercept and the ΔH is determined from the slope.

Figure 3 shows a plot of free energy vs number of fluorine atoms for compounds **6a**−**e**, Table 2. The general trend is such that more fluorine substitution leads to higher attractive interac-

(28) Leffler, J. E.; Grunwald, E. *Rates and equilibria of organic reactions as treated by statistical, thermodynamic, and extrathermodynamic methods*; Wiley: New York, 1963.

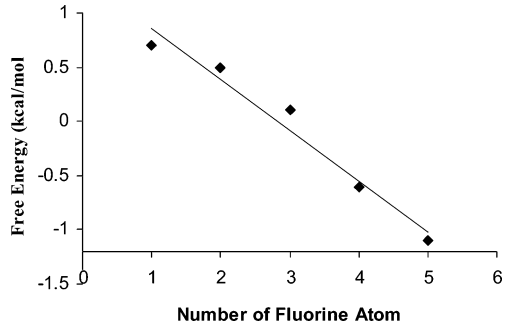

FIGURE 3. Plot showing the trend in stacking free energy for compounds **6a**−**e** as a function of the number of fluorine substitutions on Ar_2 ($Ar_1 = C_6H_4NMe_2$). Primary data are given in Tables 1 and 2.

tion. This trend follows the reasoning that electrostatic forces dominate the interactions. The quadrupole moments of the fluorinated aromatic rings gradually change from negative to positive as the number of fluorine atoms increases.[17] It follows that attractive interactions occur between the tetra- and pentafluorinated arene and the $Me_2NC_6H_4$ group while either repulsive interactions occur between the mono-, di-, and trifluorinated benzoate and the $Me_2NC_6H_4$ group or the anti conformation becomes attractive in the latter three model compounds. It is interesting to note that although the enthalpies of compounds **6c** (Ar_2 = trifluorophenyl) and **6d** (Ar_2 = difluorophenyl) have negative signs, the free energies have positive signs, meaning that entropic effects may play a role for these two compounds.

The trend in Figure 3 is also consistent with a donor−acceptor mechanism, in which the donor is the $C_6H_4NMe_2$ group and the acceptors are fluorinated benzoate groups. As the acceptor becomes more electron-deficient, the interaction becomes stronger. The pentafluoro substitution has a stronger attractive interaction than the trend line would predict. A UV band at 318 nm was observed for compound **6a**, which was absent in the precursors' spectra. None of the other model compounds showed such UV absorption. We attribute this to charge-transfer interactions. It is consistent with our previous suggestion that in order to observe a charge-transfer band in the UV spectrum, a certain threshold of a high HOMO for the donor and low LUMO for the acceptor must be met to narrow the energy gap between the donor and the acceptor. When the arene is a relatively weak acceptor,[21] such as the pentafluorobenzoate group, it appears that the donor must be at least as electron rich as an *N*,*N*-dimethylaminophenyl group.

Anti conformation was dominant for all compounds studied where Ar_1 is either a phenyl or a nitrophenyl group except where $Ar_2 = C_6F_5$ or $C_6H_4NO_2$ (Table 3). This is in contrast to our recent report on parallel displaced models,[16] where most arenes prefer the syn conformation. The only favorable syn conformation in the current models is when $Ar_2 = C_6F_5$ or $C_6H_4NO_2$. Two possible reasons can account for the difference. The first possibility is that sandwich configuration between two aromatic rings is repulsive unless one of the arenes is reasonably electron-deficient. The second possibility is that the imperfect edge-to-face interaction in the anti conformation plays a role in the syn−anti equilibrium. Currently we prefer the first explanation because the highest anti preference (anti/syn = 8.3) is exhibited by model compound **7h** where $Ar_1 = C_6H_5$ and $Ar_2 = C_6H_4CH_3$ rather than compound **8g** (anti/syn = 2.3) where $Ar_1 = C_6H_4NO_2$ and $Ar_2 = C_6H_4CH_3$. If the edge-to-face interaction in the anti conformation plays a dominant role, one would expect

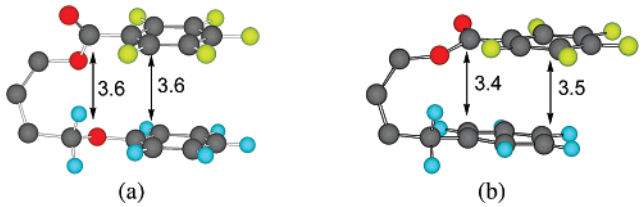

FIGURE 4. Chem3D representations of (a) sandwich and (b) parallel-displaced models with the triptycene skeleton omitted for clarity. Structures were optimized with use of MacroModel (version 7.0, force field: MMFFs). Interplanar distances are labeled in angstroms.

8g has a higher anti preference because the nitro group increases the phenyl CH acidity.

A comparison of the observed ratios of *syn* vs *anti* isomers for the two different model systems is summarized in Table 4. The energy-optimized structures for the two models with C_6F_5 and C_6H_5 are shown in Figure 4 (with the triptycene skeleton omitted for clarity). The parallel-displaced model has a smaller interplanar distance. In general, the parallel-displaced models give a greater percentage of *syn* isomers. When one arene is the strongly electron-deficient pentafluorophenyl group, both models prefer the *syn* conformation significantly, but by a comparable margin. The general trend in the attractive stacking interaction toward a pentafluorobenzoate is consistent with a donor−acceptor relationship. For example, the order of preference for the syn conformation is $Me_2NC_6H_4 > C_6H_5 > O_2NC_6H_4$ and in the multi-methyl series the order of preference is $Me_3C_6H_2 > Me_2C_6H_3 > MeC_6H_4 > C_6H_5$. The observed trend applies when the acceptor is a C_6F_5CO group. When $Ar_1 = C_6H_4OMe$, the syn/anti ratio is smaller than expected. This may be explained by considering the sandwich structure in the syn conformation. In the stacked conformation, the oxygen atom of the methoxy substituent is in close proximity to a fluorine atom from the C_6F_5, which causes repulsive interactions. The fact that a charge-transfer band is observed for compound **6a**, where $Ar_1 = Me_2NC_6H_4$ and $Ar_2 = C_6F_5$, supports the notion that donor−acceptor interactions play a role.

A much greater difference in syn/anti ratio between the two configurations is observed when neither of the arenes is strongly electron-deficient. In these cases, the ratio of the syn/anti isomers for the parallel-displaced model is greater than three times that of the sandwich model. The sandwich model shows a much greater preference for the anti isomer indicating either a greater repulsive interaction in the *syn* conformation or a potential attractive interaction in the *anti* conformation although less likely.

Considering the data in whole, we interpret these results by a combination of electrostatic, London dispersive, and charge-transfer effects. When one arene is the strongly electron-deficient pentafluorophenyl group, the dominant role is played by electrostatic (including quadrupolar/dipolar) interactions which exist in both sandwich and the parallel-displaced configurations. In addition donor−acceptor interactions also play a role as evidenced by the substituent effects and the observation of a charge-transfer band of compound **6a**. The parallel-displaced configuration has the advantage of allowing a closer interplanar distance, which enhances London dispersive forces.[21] This explains why the parallel-displaced configuration in general has a stronger binding energy than the sandwich configuration. When none of the arenes is strongly electron-deficient, electrostatic forces are repulsive in the sandwich configuration while attractive in the parallel-displaced configuration, which explains

why the syn/anti ratio is three times greater with the parallel-displaced configuration. Thus both electrostatic and dispersive forces favor the parallel-displaced configuration. A further argument for the role of dispersion is to point out that one would mistakenly predict a preferred sandwich conformation for $C_6F_6-C_6H_6$ interactions if quadrupole moments alone were considered. Recent theoretical studies of the $C_6F_6-C_6H_6$ complex indicate that the parallel-displaced configuration is the energy minimum even for the completely symmetrical aromatic complex.[21,29]

Summary

The triptycene-derived molecular model system has been used to quantitatively study arene−arene interactions in the near-sandwich configuration. Both enthalpy and entropy are obtained for 21 different compounds via variable-temperature NMR spectroscopy. Similar to models with arenes in the parallel-displaced configuration, arene−arene interaction in the sandwich configurations also prefers the *syn* conformation if the two arenes are of opposite polarity, i.e., one electron-rich and the other electron-poor. Overall the sandwich configuration shows a smaller attractive interaction than the parallel-displaced configuration. The electrostatic model based on quadrupole moments alone cannot completely explain the preference for the parallel-displaced arrangement. Our recent theoretical study in conjunction with our previous results has appeared, which shows that dispersive forces are important in determining the energy minimum.[21] The origin of the preference for the parallel-displaced conformation with regard to $C_6F_6-C_6H_6$ is related to the closeness of stacking.

Experimental Section

Representative Procedure for the Preparation of the Model Compounds: 9-(4-Dimethylaminophenoxymethyl)-1-(4-fluorobenzoyloxy)-4-pivaloyloxytriptycene (6e). 9-(4-(Dimethylamino)phenoxymethyl)-1-hydroxy-4-(pivaloyloxy)triptycene (**5**) (0.15 mmol) was treated with 4-fluorobenzoyl chloride (0.19 mmol) and 4-(dimethylamino)pyridine (50 mg, 0.42 mmol) in pyridine (1 mL) at ambient temperature for 24 h. Then 5 mL of 1 N HCl was added to quench the reaction. The mixture was extracted with methylene chloride and the extract was washed with aqueous HCl solution two times and dried over $MgSO_4$. The solvent was removed under reduced pressure. Further purification of the crude via flash column chromatography provided compound **6e** as a solid (96%): mp 249−251 °C; ^{1}H NMR (300 MHz, $CDCl_3$) δ 7.78−8.36 (2H, m), 7.31−7.42 (5H, m), 6.73−7.03 (7H, m), 6.50−6.52 (4H, m), 5.08−5.62 (3H, m), 2.83 (6H, s), 1.53 (9H, m); ^{13}C NMR (75 MHz, $CDCl_3$) δ 176.4, 164.1, 162.2, 144.3, 143.4, 133.2, 125.7, 125.7, 125.4, 124.6, 123.9, 121.2, 120.3, 116.5, 115.2, 66.3, 55.0, 48.5, 39.4, 32.6, 27.4; HRMS calcd for $C_{41}H_{36}FNO_5$ + H 642.2656, found 642.2655.

Variable-Temperature NMR Experimental Procedure. The ^{1}H NMR spectra were recorded on a 300 MHz instrument with a variable-temperature probe. A 0.05 M solution of the sample in a deuterated solvent such as chloroform was placed in a high-quality NMR tube. All samples were degassed by using a needle to bubble nitrogen through the sample for ∼1 min. The NMR tube was then capped with a cap and sealed with Parafilm. The sample tube was placed into the NMR probe and the air line to the probe was replaced with a liquid nitrogen transfer line. The desired temperature was set on the variable-temperature unit and the sample was allowed to equilibrate for 10−15 min at each set temperature. Then the ^{1}H NMR spectrum at each temperature was recorded. The ratios of rotamers were obtained through the integrations of selected peaks.

Acknowledgment is made to the donors of the Petroleum Research Fund (PRF#40361-AC1), administered by the American Chemical Society. We are grateful for support from the National Institutes of Health (GM069441).

Supporting Information Available: Experimental procedures for the preparation of compounds **3**−**13** and their ^{1}H NMR spectra. This material is available free of charge via the Internet at http://pubs.acs.org.

JO062526T

(29) Tsuzuki, S.; Uchimaru, T.; Mikami, M. Intermolecular interaction between hexafluorobenzene and benzene: Ab initio calculations including CCSD(T) level electron correlation correction. *J. Phys. Chem. A* **2006**, *110*, 2027−2033.